Hindawi Publishing Corporation
Journal of Nanomaterials
Volume 2014, Article ID 739485, 9 pages
http://dx.doi.org/10.1155/2014/739485

Research Article

Size-Controlled Synthesis of Fe_3O_4 Magnetic Nanoparticles in the Layers of Montmorillonite

Katayoon Kalantari, Mansor B. Ahmad, Kamyar Shameli, Mohd Zobir Bin Hussein, Roshanak Khandanlou, and Hajar Khanehzaei

Department of Chemistry, Faculty of Science, Universiti Putra Malaysia (UPM), 43400 Serdang, Selangor, Malaysia

Correspondence should be addressed to Katayoon Kalantari; ka_upm@yahoo.com and
Mansor B. Ahmad; mansorahmad@upm.edu.my

Received 9 June 2014; Accepted 4 August 2014; Published 15 September 2014

Academic Editor: Hongchen Chen Gu

Iron oxide nanoparticles (Fe_3O_4-NPs) were synthesized using chemical coprecipitation method. Fe_3O_4-NPs are located in interlamellar space and external surfaces of montmorillonite (MMT) as a solid supported at room temperature. The size of magnetite nanoparticles could be controlled by varying the amount of NaOH as reducing agent in the medium. The interlamellar space changed from 1.24 nm to 2.85 nm and average diameter of Fe_3O_4 nanoparticles was from 12.88 nm to 8.24 nm. The synthesized nanoparticles were characterized using some instruments such as transmission electron microscopy, powder X-ray diffraction, energy dispersive X-ray spectroscopy, field emission scanning electron microscopy, vibrating sample magnetometer, and Fourier transform infrared spectroscopy.

1. Introduction

In recent years, considerable attention has been paid to iron oxides, especially on magnetic (Fe_3O_4) nanoparticles due to their potential applications such as pigment, magnetic resonance imaging, magnetic drug delivery, Ferro fluids, recording material, and data storage media [1, 2]. There are many reports on the synthesis and characterization of magnetic nanoparticles; this is due to its significance in various fields, especially, when this material is made at the nanoscale. Magnetic nanoparticles have been prepared by various methods such as arc discharge, mechanical grinding, laser ablation, microemulsion, and high temperature decomposition of organic precursors [3]. However, research is still going on to obtain well-dispersed magnetic nanoparticles.

Several methods have been developed recently for preparing magnetic nanoparticles, including coprecipitation [4], sol-gel method [5], hydrothermal process [6], and the solvothermal method [7]. Among these methods, coprecipitation is considered as the simplest, most efficient, and most economic method.

However, there are three major challenges that these nanoparticles present. One is related to easy oxidation/dissolution of magnetic nanoparticles (NPs). The other two drawbacks are the difficulty in recycling such small sized NPs and coaggregation of nanoparticles in which case, leads to decrease the effective surface area of nanoparticles and thus reduce their reaction activities. In order to protect the magnetic NPs against oxidation, a shell structure is often introduced, such as a silica shell or polymer shell [8]. Several methods have been accordingly developed to minimize the coaggregation of nanoparticles, obtain the soft sediment, and improve their manipulation, such as supporting of magnetic nanoparticles on polymers or inorganic matter, like porous silica [9, 10].

Clay minerals, which are abundant and environmental friendly, are used as the supporting materials of magnetic nanoparticles. Sodium montmorillonite (Na-MMT) $(Na_{0.7}(Al_{3.3}Mg_{0.7})\ Si_8O_{20}(OH)_4.nH_2O)$, a kind of 2 : 1 type layered silicates in which each layer comprises an alumina octahedral sheet sandwiched between two silica tetrahedral sheets, is known as a polymer modifier due to its high specific surface area [11].

Such layers are stacked by weak dipolar or van der Waals forces, leading to the interaction of charge compensating cations into the interlayer space. Therefore, not only adsorption on the external surface but also intercalation into the interlayer space can occur [12].

Here we present our results obtained from synthesized magnetic nanoparticles well dispersed on montmorillonite using sodium hydroxide as a reducing agent.

2. Materials and Methods

In this work, all reagents were of analytical grade. Ferric chloride hexahydrate ($FeCl_3.6H_2O$) and ferrous chloride tetrahydrate ($FeCl_2.4H_2O$) of 96 wt. % were used as the iron precursors and also montmorillonite powder was obtained from (Kunipia-F, Tokyo, Japan). NaOH of 99 wt. % was obtained from Merck KGaA (Darmstadt, Germany). All solutions were freshly prepared using deionized water.

2.1. Fe_3O_4/Montmorillonite NCs Preparation. The Fe_3O_4 nanoparticles were synthesized using chemical coprecipitation method. Prior to use, all glassware used in experimental procedures were cleaned in a fresh solution of HNO_3/HCl (3 : 1, v/v), washed thoroughly with double distilled water, and dried. For the synthesis of Fe_3O_4/montmorillonite nanocomposites (Fe_3O_4/MMT NCs), different volumes of deionized water were bubbled by N_2 gas for 15 min and then 2.0 g of montmorillonite and measured amount of Fe^{3+} and Fe^{2+} with a molar ratio of 1 : 2 were successively dissolved in ultrapure water with vigorous mechanical stirring for 2 hours. Under the protection of nitrogen gas, 1.50, 3.0, 5.0, 7.50, 9.50, and 12.50 mL of 2 M NaOH were added dropwise into the above solutions. Eventually the Fe_3O_4-NPs content of the MMT matrix was 1.0, 3.0, 5.0, 7.0, 9.0, and 12.0 wt. %, respectively. After that, the mechanical stirrer was switched off and Fe_3O_4-NPs settled gradually. The suspensions were finally centrifuged, washed twice with ethanol and distilled water, and kept in a vacuum stove at 100°C.

2.2. Characterization. The structures of the synthesized Fe_3O_4-NPs in MMT were examined using Philips X'pert PXRD (copper Kα radiation; PANalytical, Almelo, The Netherlands). The changes in the interlamellar spacing of MMT were also studied by using PXRD in the small-angle range of 2θ (5–15 degrees). The scan speed of 2 degrees/minutes was applied to PXRD patterns recording. TEM images of the samples were recorded with an H-7100 electron microscope (Hitachi Ltd., Tokyo, Japan). The samples were prepared by dispersing about 0.1 g powder with 8 mL ethanol by ultrasound for 20 min. A drop of the dispersion was applied to a holey carbon TEM support grid. Excess solution was blotted off using a filter paper. The analysis of the surface morphologies of the samples was performed with an (XL 30; Philips) environmental scanning electron microscope (SEM). The cleaned and dried samples were first coated with gold using sputter coater. For elemental analysis of the nanoparticles, energy dispersion X-ray spectroscopy was carried out on a Shimadzu EDX-700HS spectrometer attached to the SEM. The FTIR spectrum was used to identify the functional groups present in the synthesized compound. FTIR spectra were recorded over the range of 200–4000 cm^{-1} utilizing the Series 100 FTIR 1650 spectrophotometer (PerkinElmer, Waltham, MA, USA). Magnetization measurements were carried out with a Lakeshore (model 7407) vibrating sample magnetometer (VSM) to study magnetic properties of the Fe_3O_4 nanoparticles under magnetic field up to 10 kG at room temperature.

3. Results and Discussion

The customized shape and size of prepared magnetic nanoparticles have been a challenge in scientific and technological issues. The wet chemical methods to magnetic nanoparticles are more effective and simpler with good control over composition and size [13]. Fe_3O_4-NPs can be prepared through the coprecipitation of Fe^{3+} and Fe^{2+} aqueous salts solution by addition of base as reducing agent. The chemical reaction may be presented as follows [14]:

$$Fe^{2+}/Fe^{3+}/MMT + 8OH^- \longrightarrow Fe_3O_4/MMT\ NCs + 4H_2O. \quad (1)$$

The surface of MMT is assisting the Fe_3O_4-NPs nucleation during the reduction process. The schematic illustration of the synthesis of Fe_3O_4/MMT NCs from MMT/Fe^{3+}–Fe^{2+} suspension produced by using sodium hydroxide is shown in Figure 1. Meanwhile, as shown in Figure 2, the MMT suspension was gray (a) and the addition of Fe^{3+}–Fe^{2+} ions to the MMT change color to the light brown (b), brown (c), and dark brown (d) for 1.0, 7.0, and 12.0 wt. %, respectively, but after the addition of NaOH to the suspensions they turned to black color (e), (f), and (g) that indicate the abundance of Fe_3O_4-NPs in the MMT suspensions.

3.1. Powder X-Ray Diffraction. The basal spacing of MMT (Figure 3(a)) was 1.24 nm at $2\theta^\circ$, 8.83°. Combination with Fe_3O_4 NPs expanded the basal spacing to 1.47, 1.68, 1.87, 2.10, 2.53, and 2.85 nm at the $2\theta^\circ$, 8.75°, 8.66°, 8.51°, 8.21°, 7.72°, and 7.46° in 1.0, 3.0, 5.0, 7.0, 9.0, and 12.0 wt. %, respectively. It may be assumed that the iron ions penetrated into the interlayer space of montmorillonite via ion-exchange and were reduced by NaOH to Fe_3O_4 NPs. In this case, the interlayer space would have acted as a size controller and microreactor [15]. Moreover the intensities of the reflections were significantly decreased, and the highly ordered parallel lamellar structure of the MMT was disrupted by the Fe_3O_4-NPs formation [16]. Figure 3(b) reveals X-ray diffraction patterns of prepared Fe_3O_4-NPs. The reflections of Fe_3O_4-NPs at $2\theta^\circ$, 31.62°, 35.78°, 43.84°, 59.67°, 62.53°, and 74.58° are related to the 220, 311, 400, 511, 440, and 622 crystalline structure with a spinel structure. Comparing XRD pattern of synthesized NPs with the standard diffraction spectrum (ref. code Fe_3O_4:01-088-0315), the synthesized product is crystalline Fe_3O_4 [17]. The size of Fe_3O_4-NPs is significantly influenced by the kind of reducing agent used in the reaction. Generally, a strong

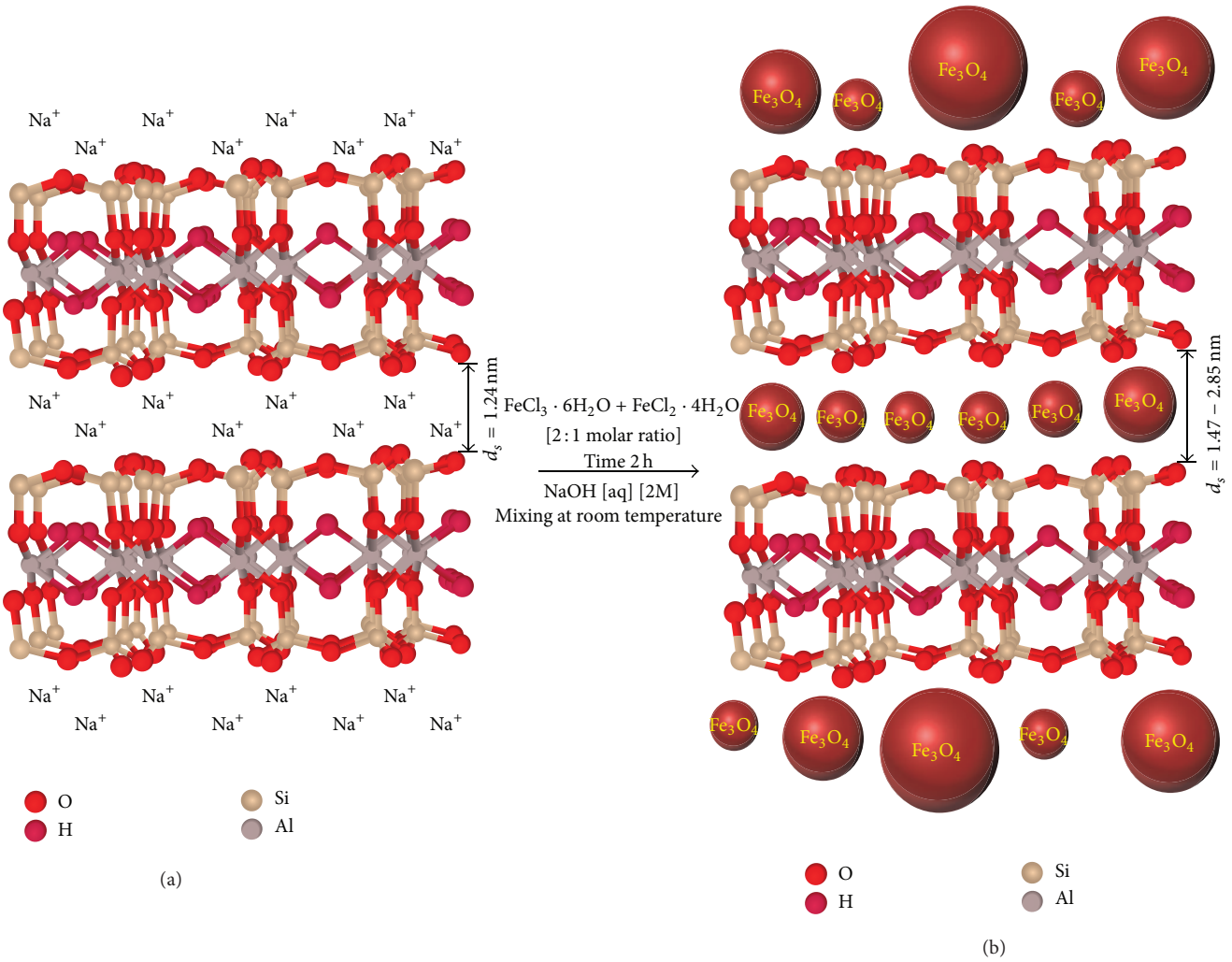

Figure 1: Schematic illustration of the synthesized Fe_3O_4-NPs in the interlayer space of MMT suspension by chemical coprecipitation reduction method ((a)-(b)).

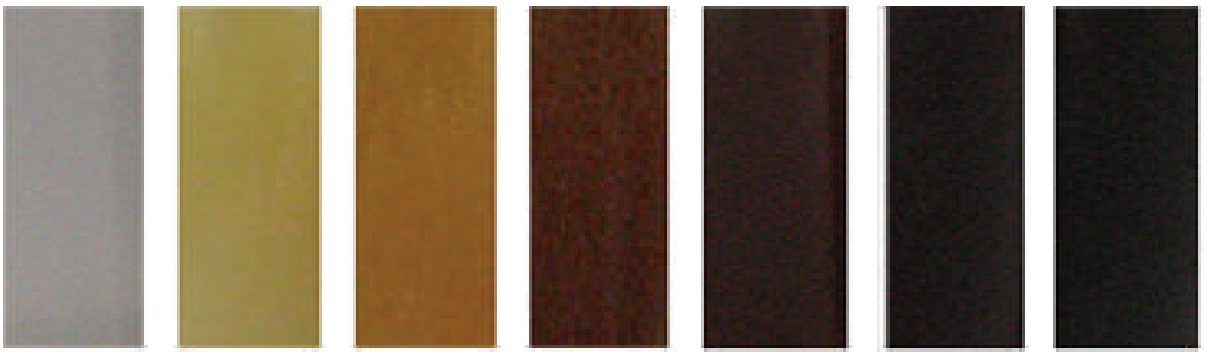

Figure 2: Photograph of montmorillonite suspension (a) and Fe^{2+}/Fe^{3+}/MMT suspension at different Fe^{2+}/Fe^{3+}/concentrations; (b) 1.0%, (c) 7.0%, (d) 12.0% and Fe_3O_4/MMT NCs, (e) 1.0%, (f) 7.0%, and (g) 12.0%.

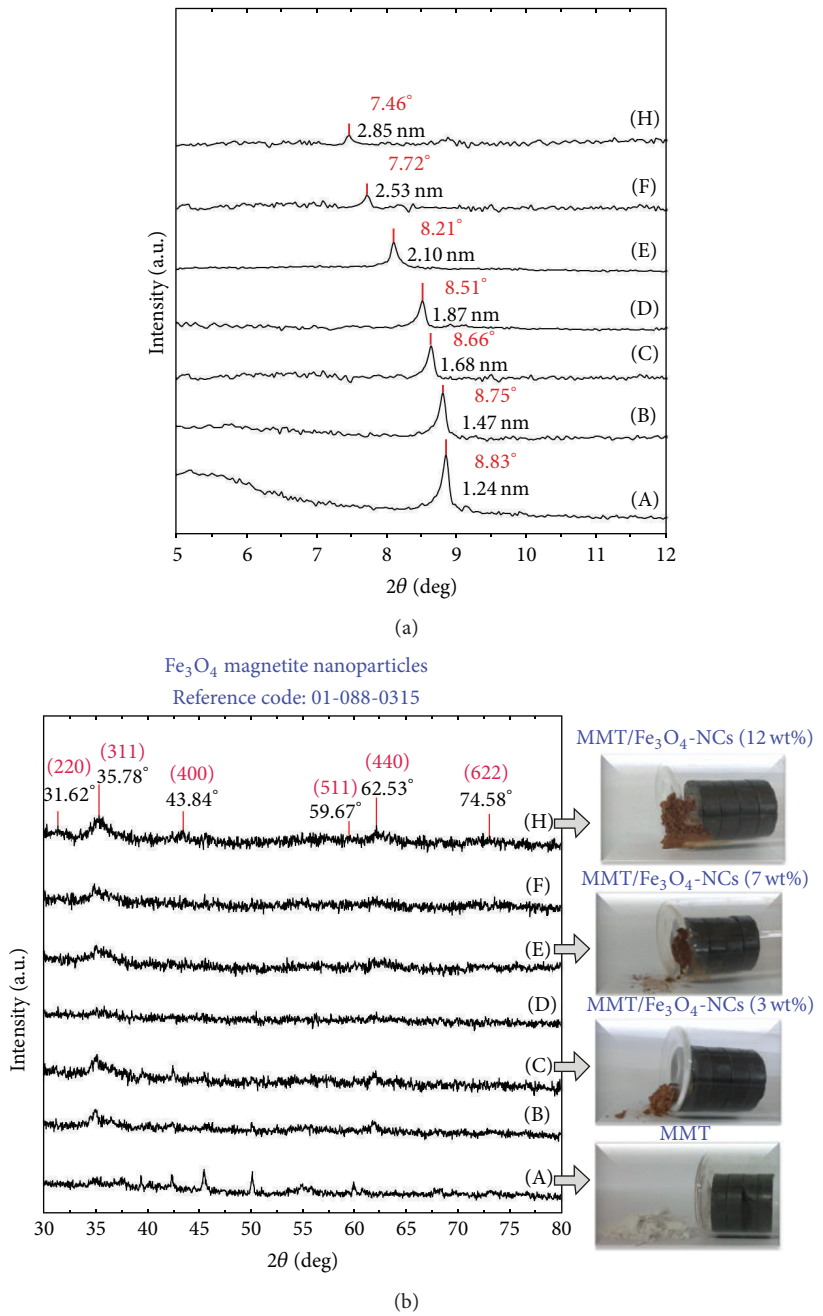

FIGURE 3: (a) Powder X-ray diffraction patterns of MMT (a) and Fe_3O_4/MMT NCs for determination of d-spacing (d_s) and crystals structure at different percentage of NPs (1.0, 3.0, 5.0, 7.0, 9.0, and 12.0 wt. % ((b)–(f))). (b) Powder X-ray diffraction patterns of MMT (a) and MMT–Fe_3O_4-NCs for determination of Fe_3O_4 crystal structure. (b)–(h): 1, 3, 5, 7, 9, and 12% (w/w).

reducing agent promotes a fast rate and favors the formation of smaller NPs. Meanwhile, we have found that the amount of NaOH has a significant effect on the size of Fe_3O_4-NPs [18] and increasing the NaOH amount will lead up to the decrease of Fe_3O_4-NPs size gradually. The possible reason is that repulsive force between hydroxide ions hinders the growth of crystal grains when the excess hydroxide ions produced from NaOH are adsorbed on the surface of crystal nuclei [19]. Additionally, as shown in Figure 3(b), Fe_3O_4/MMT NCs, 12.0 wt. %, completely absorbed when exposed to an external magnetic field, and the response decreased with the decreasing in Fe_3O_4 percentage.

3.2. Transmission Electron Microscopy (TEM). Figure 4 shows TEM images of Fe_3O_4-NPs in the interlayer space or on the montmorillonite surface. The size distribution histograms of Fe_3O_4/MMT NCs in Figures 4(a)–4(d) were determined by measuring the diameter of 8.24, 10.38, 12.57, and 12.88 nm for 1.0, 5.0, 9.0, and 12.0 wt. %, respectively. Due

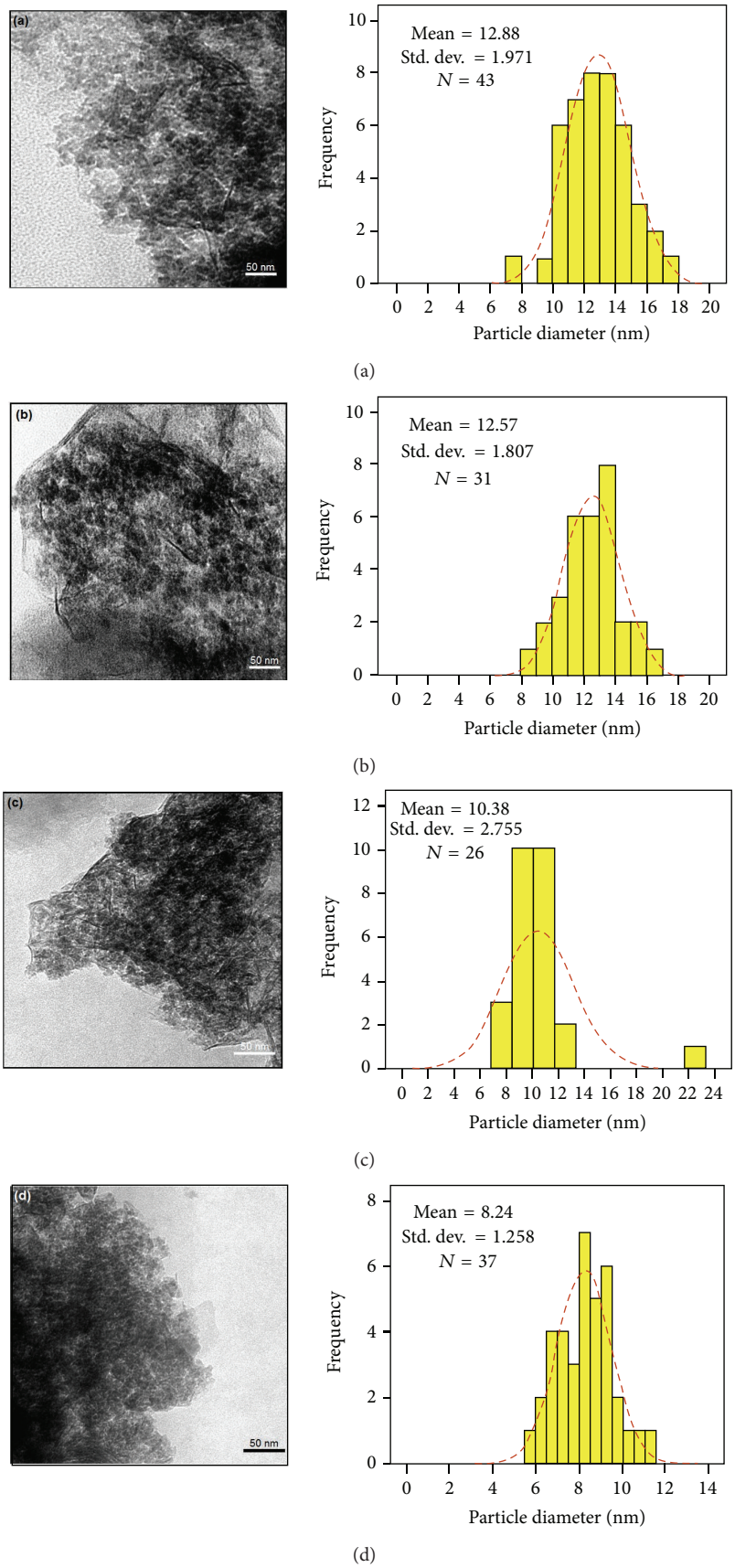

FIGURE 4: The transmission electron microscopy images and particle size distribution histogram for 1.0, 5.0, 9.0, and 12.0 wt. % of the Fe_3O_4/MMT NCs.

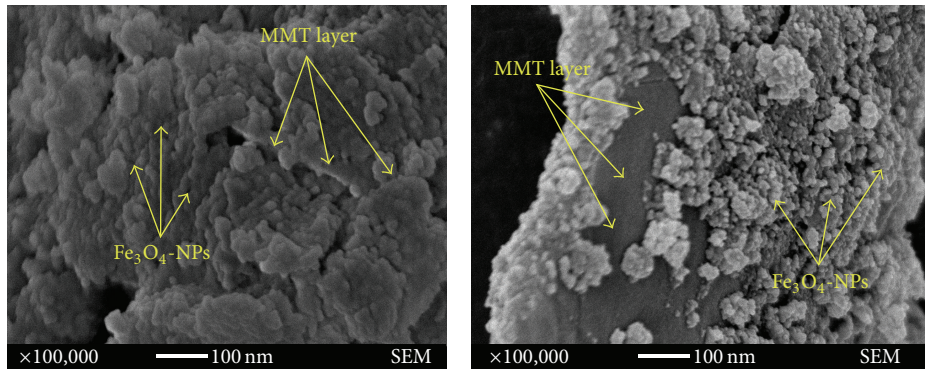

(a) (b)

Figure 5: The scanning electron microscopy micrographs of Fe_3O_4/MMT NCs with high magnification for 1.0 and 12.0 wt. % (a) and (b).

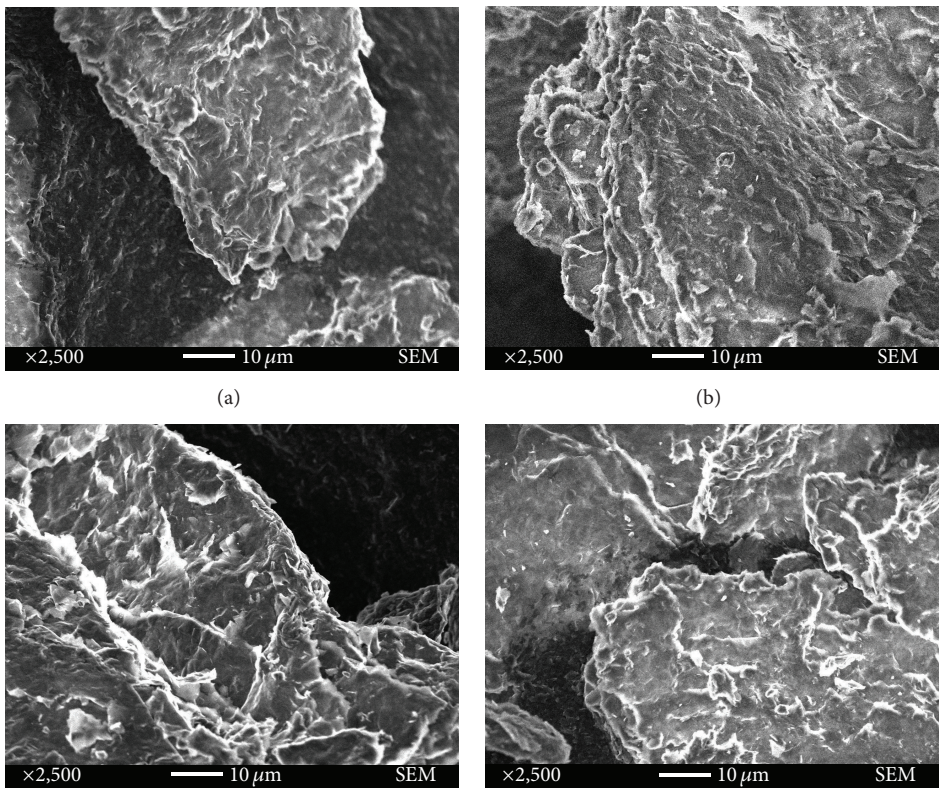

(a) (b)

(c) (d)

Figure 6: The scanning electron microscopy micrographs of MMT (a) and Fe_3O_4/MMT NCs for 5.0, 9.0, and 12.0 wt. % (b), (c), and (d).

to the high density of ion-exchange sites on MMT, the highly charged Fe_3O_4-NPs are strongly bound via electrostatic interaction to the surface. The higher abundance of NPs aggregates in the MMT composite is in direct correlation with the smaller primary NPs dimensions [20].

3.3. Scanning Electron Microscopy (SEM). SEM images show that the Fe_3O_4-NPs are in spherical shape (Figures 5(a) and 5(b)). Fe_3O_4-NPs have very high surface free energy, which lead to instability in their dispersions thermodynamic system; stability is restored upon Ostwald ripening [21]. The isotopic nucleation rate per unit area at the interface between the Fe_3O_4-NPs leads to forming the spherical shape NPs due to equivalent growth rate along every direction of the nucleation as the sphere has the smallest surface area per unit volume compared to other shapes [22]. Figure 6 clearly shows that the size of Fe_3O_4-NPs in 1.0 wt. % sample is smaller than 12.0 wt. % which is in line with the TEM and XRD results previously mentioned.

A general view of the MMT with a typical sheet-like structure with large flakes can be observed in Figure 6(a)

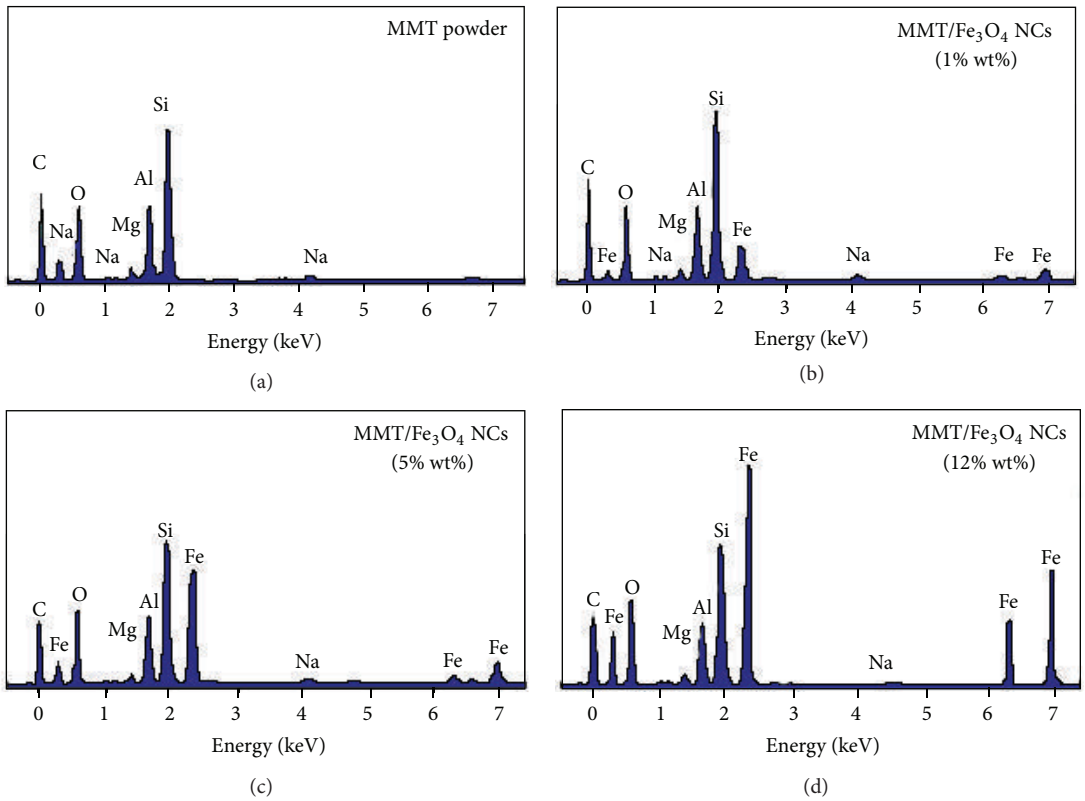

Figure 7: Energy dispersive X-ray spectroscopy of MMT (a) and Fe_3O_4/MMT NCs for 1.0, 5.0, and 12.0 wt. % (b), (c), and (d).

and it confirmed that the small difference can be observed in morphology structure of MMT compared with Fe_3O_4/MMT NCs (Figures 6(b)-6(c)). The different brightness of the MMT and MMT supported Fe_3O_4-NPs and some disordering in the MMT structure are due to the abundance of iron oxide coating on the surface of clay.

3.4. Energy Dispersive X-Ray Spectroscopy (EDX). The oxygen and iron peaks in EDX spectrum reveal the existence of Fe_3O_4-NPs (Figure 7). In Figure 7(a), the peaks around 1.7, 2.7, 2.9, 3.7, 4.0, 4.5, 6.4, and 7.1 keV are related to the binding energies of MMT. The peaks around 0.2, 2.2, 6.4, and 7.0 keV are related to Fe_3O_4-NPs elements, respectively, in Figures 7(b)–7(d) [20]. Moreover, with an increase amount of iron oxide, the iron peaks height increases in the Fe_3O_4/MMT NCs (1.0, 5.0, and 12.0 wt. wt. %). Additionally, the EDXRF spectra for the MMT and for Fe_3O_4/MMT NCs confirm the presence of elemental compounds in the MMT and Fe_3O_4-NPs without any impurity peaks. The results indicate that the synthesized Fe_3O_4-NPs are in high purity.

3.5. FTIR Chemical Analysis. For pure MMT, the bending mode of Al-Al-OH is found at 910 cm^{-1} because of the large amount of Al in the octahedral site of oxygen and the bending mode of Si-O-Al was observed at 513 cm^{-1}. The band at 3633 cm^{-1} (Figure 8(a)) that identified stretching vibration of the structural hydroxyl group of MMT was detected [23]. Figures 8(b)–8(f) show that there were no many changes in

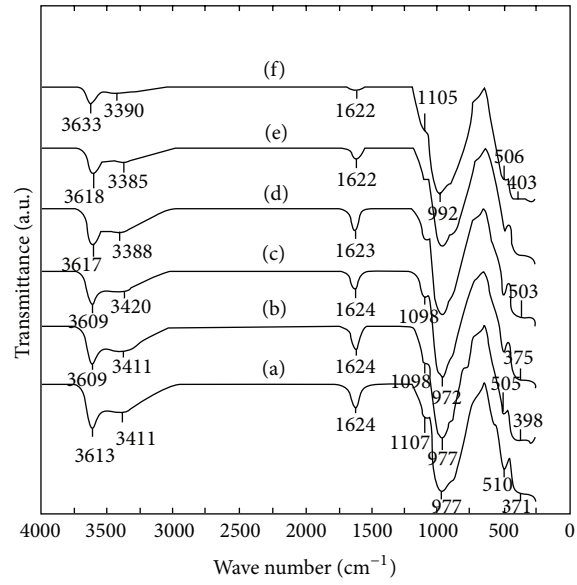

Figure 8: FTIR spectra of MMT (a) and Fe_3O_4/MMT NCs (b), (c), (d), (e), and (f).

the spectra of Fe_3O_4/MMT NCs compared with MMT. The bands between 446 cm^{-1} and 625 cm^{-1} can be assigned to Fe-O stretching vibration which may be due to the overlapping of Si-O and Al-OH.

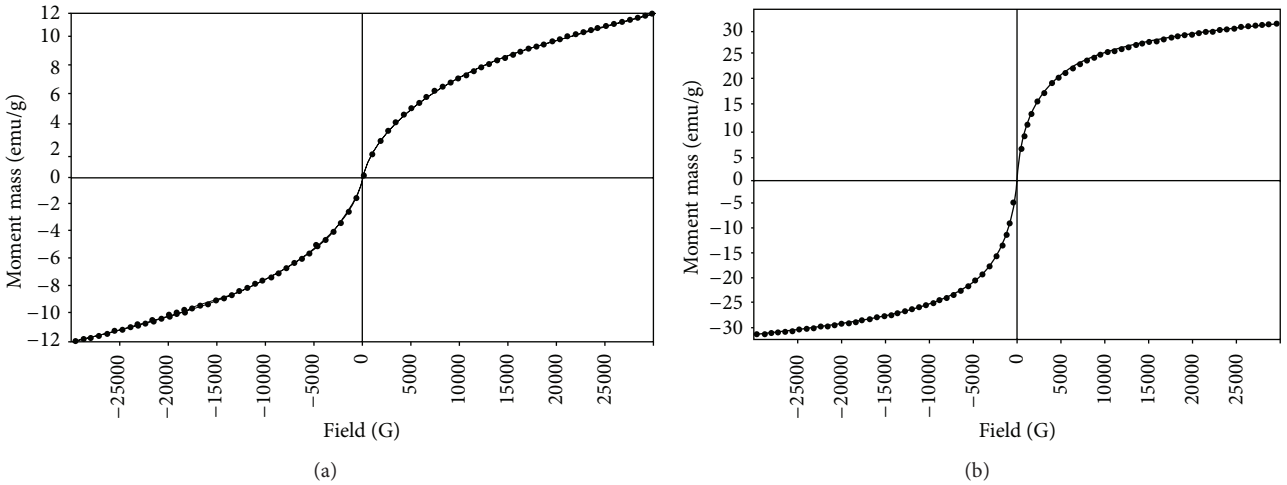

Figure 9: Magnetization curve of Fe_3O_4/MMT NCs 1.0% (a) and 12.0% (b).

The FTIR spectra demonstrated the inflexibility of silicate layers and nonbond chemical interface between the silicate layers and Fe_3O_4-NPs in Fe_3O_4/MMT NCs. These results confirmed that, with an increase amount of Fe_3O_4-NPs in the Fe_3O_4/MMT NCs due to the existence of van der Waals interactions between the oxygen groups of MMT and Fe_3O_4-NPs, peak areas shifted to low wave numbers and the intensity of peaks decreased [16].

3.6. Vibrating Sample Magnetometer (VSM). The vibrating sample magnetometer (VSM) was applied to test the magnetic properties of Fe_3O_4/MMT NCs. The magnetization curves for Fe_3O_4/MMT NCs in 1.0 and 12.0 wt. % are shown in Figure 9. It can be seen from the magnetization curves that the saturation magnetization (Ms) of the Fe_3O_4/MMT NCs increased from 12.10 to 32.40 emu.g^{-1} when Fe_3O_4 content increased from 1.0 to 12.0 wt. % of composite. It indicated more Fe_3O_4 being trapped in the MMT layers.

4. Conclusion

In this work, we synthesized successfully Fe_3O_4/MMT NCs through coprecipitation method which is a cheap, facile, and environmental friendly method. Sodium hydroxide was used as reducing agent and ferric chloride and ferrous chloride were used as the iron precursors. These synthesized Fe_3O_4-NPs with high magnetization and good dispersion are on the external surface and between the layers of montmorillonite. Our results show that the amount of NaOH (reducing agent) has significant effect on the size of nanoparticles. Smaller sized nanoparticles were obtained due to more reducing agent amount. Moreover, these results indicate that montmorillonite used here can act as an effective support for the synthesis of magnetic nanoparticles.

The specific surface areas of Fe_3O_4/MMT NCs were larger than pure montmorillonite. The comparison between the PXRD patterns of MMT and the prepared Fe_3O_4/MMT NCs indicated the immobilized formation of Fe_3O_4-NPs in the interlamellar space of the MMT layers. The TEM images showed that the mean diameter of the nanoparticles ranged from 8.24 nm to 12.88 nm.

Conflict of Interests

The authors declare that there is no conflict of interests regarding the publication of this paper.

Acknowledgments

The authors would like to acknowledge the financial support from Universiti Putra Malaysia (UPM) (RUGS Project no. 9199840). They are also grateful to the staff of the Department of Chemistry, UPM, and the Institute of Bioscience, UPM, for the technical assistance.

References

[1] G. Mihoc, R. Ianoş, C. Păcurariu, and I. Lazău, "Combustion synthesis of some iron oxides used as adsorbents for phenol and p-chlorophenol removal from wastewater," *Journal of Thermal Analysis and Calorimetry*, vol. 112, no. 1, pp. 391–397, 2013.

[2] M. Abbas, B. Parvatheeswara Rao, S. M. Naga, M. Takahashi, and C. Kim, "Synthesis of high magnetization hydrophilic magnetite (Fe_3O_4) nanoparticles in single reaction—surfactantless polyol process," *Ceramics International*, vol. 39, no. 7, pp. 7605–7611, 2013.

[3] F. Ahangaran, A. Hassanzadeh, and S. Nouri, "Surface modification of Fe_3O_4@SiO_2 microsphere by silane coupling agent," *International Nano Letters*, vol. 3, no. 1, pp. 1–5, 2013.

[4] N. Wang, L. Zhu, D. Wang, M. Wang, Z. Lin, and H. Tang, "Sono-assisted preparation of highly-efficient peroxidase-like Fe_3O_4 magnetic nanoparticles for catalytic removal of organic pollutants with H_2O_2," *Ultrasonics Sonochemistry*, vol. 17, no. 3, pp. 526–533, 2010.

[5] K. Raja, S. Verma, S. Karmakar, S. Kar, S. J. Das, and K. S. Bartwal, "Synthesis and characterization of magnetite nanocrystals," *Crystal Research and Technology*, vol. 46, no. 5, pp. 497–500, 2011.

[6] S. Ahmadi, C.-H. Chia, S. Zakaria, K. Saeedfar, and N. Asim, "Synthesis of Fe_3O_4 nanocrystals using hydrothermal approach," *Journal of Magnetism and Magnetic Materials*, vol. 324, no. 24, pp. 4147–4150, 2012.

[7] G. Gao, R. Shi, W. Qin et al., "Solvothermal synthesis and characterization of size-controlled monodisperse Fe_3O_4 nanoparticles," *Journal of Materials Science*, vol. 45, no. 13, pp. 3483–3489, 2010.

[8] G. Li, Z. Zhao, J. Liu, and G. Jiang, "Effective heavy metal removal from aqueous systems by thiol functionalized magnetic mesoporous silica," *Journal of Hazardous Materials*, vol. 192, no. 1, pp. 277–283, 2011.

[9] I. Larraza, M. López-Gónzalez, T. Corrales, and G. Marcelo, "Hybrid materials: magnetite-polyethylenimine-montmorillonite, as magnetic adsorbents for Cr(VI) water treatment," *Journal of Colloid and Interface Science*, vol. 385, no. 1, pp. 24–33, 2012.

[10] B. C. Munoz, G. W. Adams, V. T. Ngo, and J. R. Kitchin, "Stable magnetorheological fluids," Google Patents, 2001.

[11] A. K. Mishra, S. Allauddin, R. Narayan, T. M. Aminabhavi, and K. V. S. N. Raju, "Characterization of surface-modified montmorillonite nanocomposites," *Ceramics International*, vol. 38, no. 2, pp. 929–934, 2012.

[12] M. Fan, P. Yuan, J. Zhu et al., "Core-shell structured iron nanoparticles well dispersed on montmorillonite," *Journal of Magnetism and Magnetic Materials*, vol. 321, no. 20, pp. 3515–3519, 2009.

[13] A. K. Gupta and M. Gupta, "Synthesis and surface engineering of iron oxide nanoparticles for biomedical applications," *Biomaterials*, vol. 26, no. 18, pp. 3995–4021, 2005.

[14] M. Zhang, G. Pan, D. Zhao, and G. He, "XAFS study of starch-stabilized magnetite nanoparticles and surface speciation of arsenate," *Environmental Pollution*, vol. 159, no. 12, pp. 3509–3514, 2011.

[15] S. Li, P. Wu, H. Li et al., "Synthesis and characterization of organo-montmorillonite supported iron nanoparticles," *Applied Clay Science*, vol. 50, no. 3, pp. 330–336, 2010.

[16] K. Shameli, M. B. Ahmad, M. Zargar, W. M. Z. W. Yunus, A. Rustaiyan, and N. A. Ibrahim, "Synthesis of silver nanoparticles in montmorillonite and their antibacterial behavior," *International Journal of Nanomedicine*, vol. 6, pp. 581–590, 2011.

[17] K. Kalantari, M. B. Ahmad, K. Shameli, and R. Khandanlou, "Synthesis of talc/Fe_3O_4 magnetic nanocomposites using chemical co-precipitation method," *International Journal of Nanomedicine*, vol. 8, pp. 1817–1823, 2013.

[18] H. Maleki, A. Simchi, M. Imani, and B. F. O. Costa, "Size-controlled synthesis of superparamagnetic iron oxide nanoparticles and their surface coating by gold for biomedical applications," *Journal of Magnetism and Magnetic Materials*, vol. 324, no. 23, pp. 3997–4005, 2012.

[19] H. Yan, J. Zhang, C. You, Z. Song, B. Yu, and Y. Shen, "Influences of different synthesis conditions on properties of Fe_3O_4 nanoparticles," *Materials Chemistry and Physics*, vol. 113, no. 1, pp. 46–52, 2009.

[20] T. Szabó, A. Bakandritsos, V. Tzitzios et al., "Magnetic iron oxide/clay composites: effect of the layer silicate support on the microstructure and phase formation of magnetic nanoparticles," *Nanotechnology*, vol. 18, no. 28, Article ID 285602, 2007.

[21] S. Hribernik, M. Sfiligoj-Smole, M. Bele, S. Gyergyek, J. Jamnik, and K. Stana-Kleinschek, "Synthesis of magnetic iron oxide particles: development of an in situ coating procedure for fibrous materials," *Colloids and Surfaces A: Physicochemical and Engineering Aspects*, vol. 400, pp. 58–66, 2012.

[22] D. K. Kim, M. Mikhaylova, Y. Zhang, and M. Muhammed, "Protective coating of superparamagnetic iron oxide nanoparticles," *Chemistry of Materials*, vol. 15, no. 8, pp. 1617–1627, 2003.

[23] Y. H. Son, J. K. Lee, Y. Soong, D. Martello, and M. Chyu, "Structure-property correlation in iron oxide nanoparticle-clay hybrid materials," *Chemistry of Materials*, vol. 22, no. 7, pp. 2226–2232, 2010.